The Indonesian Journal of Geography, Vol. 15—16, Nos. 49—51.
June 1985—June 1986, pp. 33—68

# GEOGRAPHY WITH THE ENVIRONMENTAL SATELLITES

by
J.P. Gastellu-Etchegorry*

## ABSTRACT

*Coarse spatial resolution, high temporal frequency data from the earth polar orbiting (NOAA, HACMM, Nimbus, etc.) satellites and from the geostationary (GOES, Meteosat, and GMS) satellites are presented to demonstrate their utility for monitoring terrestrial and atmospheric processes. The main characteristics of these satellites and of the instruments on board are reviewed. In order to be useful for environmental assessments, the remotely sensed data must be processed (atmospheric and geometric corrections, etc.). The NOAA Center provides a wide range of already processed data, such as meteorological, oceanic, hydrologic and vegetation products; a rough description of these preprocessed data is given in this article. Finally, some examples of applications in Southeast Asia and especially in Indonesia, are described, i.e.: agroecosystem, drought and oceanic monitoring. The paper concludes that coarse resolution, high temporal frequency satellite data are very valuable for environmental studies, the emphasis being laid on the improvement of the crop and drought assessment programmes.*

## INTRODUCTION

Knowledge of environmental and superficial earth changes requires the

* Dr. J.P. Gastellu-Etchegorry is French Project specialist in Remote Sensing at the PUSPICS (Training Centre for Image Interpretation and Integrated Surveys), UGM-BAKOSURTANAL, Faculty of Geography, Gadjah Mada University, Yogyakarta, Indonesia.

understanding and quantification of terrestrial processes on a large scale, such is the case for the influence of the sulphur cycle on the soil acidity. The importance, for many various routine tasks (weather forecasting, fishery, etc.), of the terrestrial measurements on a large scale will be stressed. Better spatial and spectral resolution, however, is necessary in order to improve the mapping and measuring of the quasi-static aspects of the earth. Furthermore, time-varying phenomena must be considered systematically over long time periods: vegetation, snow cover, sea ice, water sediments and suspended organisms, surface energy balance quantities, soil moisture, precipitation, etc.

Remote Sensing is a very good tool to satisfy these requirements. In providing the view and coverage on regional to global scales there is seldom any substitute for satellites as observational systems. However, each orbit which satellites can follow provides a unique combination of temporal and spatial coverage. Low-earth orbits provide a relatively close-up view suitable for active measurement techniques (radar and lidar) and facilitate high spatial resolution observations. The inclination of the orbital plane determines the relative balance between the extent of the coverage and the frequency of observation (see Annex). A purely equatorial orbit provides an overpass of a given location roughly every hundred minutes, but misses all of the earth which cannot be seen from directly over the equator. A nearly polar, sun-synchroneous orbit provides coverage of virtually the entire surface of the earth but only at two fixed times a day. This orbit is often chosen for Earth observations and is particularly appropriate for observing phenomena which are sufficiently persistent to permit observation only every twelve or twenty four hours. It provides near global coverage and relatively consistent illumination conditions, but virtually all observations are made at two fixed local times. Day and night contrasts can be measured, but the full cycle of diurnal variations is not sampled. This can greatly bias measurements of rapidly changing phenomena.

As the altitude of an orbit is increased, the ability to see more of the earth increases, but the size of the instrument optics required to achieve a given resolution grows. The period of the orbit also increases with altitude, so that at an altitude of roughly 35.800 km the orbital period is one day, and equatorially orbiting satellites stay over the same location on the earth's surface at all times. The orbit is geostationary and provides coverage of a region roughly one-fifth of the planet between 60 degrees north and south latitudes. This is an ideal situation for observing short time-scale phenomena and for sampling at all times of day. In this way the geostationary orbit is an excellent complement to the sun-synchroneous low earth orbit. There are also useful orbits in between. The temporal and spatial scales required by the observation, together with the type of instrument needed, dictate which orbit is suitable; there is no single ideal orbit.

According to the parameters of the analysis, different levels of observation must be considered; for instance, a good spatial resolution is not usually required for the study of the sea-surface temperature. So, according to the objectives, different types of instruments and satellites must be chosen. Hereafter the high spatial resolution satellites (Landsat and SPOT) are not considered. The emphasis is laid on satellites which provide routine informations on a large-scale basis; they are often characterised by a coarse ground resolution and a high temporal repetitivity. The environmental satellites are operated in two basic types of orbits polar orbiting and geostationary orbiting satellites.

## THE POLAR ORBITING SATELLITES

They operate in relatively low orbits, ranging from 700 to 1700 km above the earth with inclinations generally from 90 to 115 degrees. They circle the earth 12 to 14 times per day. Their orbital periods, which range from 99 to 115 minutes, are timed to allow complete global coverage twice per day; normally a day-time and a night-time view of the earth, with swaths about 2000 km in width. The corresponding environmental data are mainly provided by the NOAA and the NASA (seasat, Nimbus) satellites (Table 1).

TABLE 1: POLAR ORBITING SATELLITES

| Satellites | Asc. | Dec. | Launch date | Operational data |
|---|---|---|---|---|
| GEOS-3 | | | 4/9/75 | 4/14/75-12/1/78 |
| HCMM | 1400 | 0200 | 4/26/78 | 5/78-9/30/80 |
| Seasat | | | 6/27/78 | 7/7/78-10/9/78 |
| TIROS-N | 1500 | 0300 | 10/13/78 | 10/30/78-11/1/80 |
| Nimbus-7 | 1200 | 0000 | 10/24/78 | 10/30/78-Present |
| NOAA-6 | 1930 | 0730 | 6/27/79 | 6/27/79-6/20/83 |
| NOAA-7 | 1430 | 0230 | 6/23/81 | 8/24/81-Present |
| NOAA-8 | 1930 | 0730 | 3/28/83 | 5/3/83-6/12/84 |
| NOAA-9 | 1430 | 0230 | 12/84 | 85 |
| GEOS-4 | | | 85 | 85 |
| NOAA-10 | 1930 | 0730 | 85 | 85 |

Source: Kidwell (1985).

Note:

"Asc." is the time of ascending node in Local Solar Time (LST).
"Dec." is the time of descending node in LST.

## The NOAA Satellites

As a result of the large number of NOAA ground stations and to their low cost, NOAA data are those most suitable for many environmental analyses which do not require a high spatial resolution. The series of NOAA polar orbiting satellites that began with TIROS-1 in 1960 reached a third generation with the launch of TIROS-N in October 1978. TIROS-N has been followed by NOAA-6, 7, and 8, and further satellites in the series are planned for operation into the 1990s. The primary instruments on board these satellites are the Advanced Very High Resolution Radiometer (AVHRR) and the TIROS Operational Vertical Sounder (TOVS) complex.

### The AVHRR data

The AVHRR is a five channel scanning radiometer with channels in the visible, near-visible infrared and infrared water vapor window. They have been selected for production of quantitative sea surface temperature (STT) products, and visible and infrared imagery depicting cloud cover and thermal (Gulf Stream) features (Table 2).

TABLE 2. CHANNELS OF THE AVHRR

| Channel | NOAA-6 and 8 | NOAA-7, 9, ... | IFOV |
|---|---|---|---|
| 1 | 0.58—0.68 | 0.58—0.68 | 1.39 |
| 2 | 0.725—1.10 | 0.725—1.10 | 1.41 |
| 3 | 3.55—3.93 | 3.55—3.93 | 1.51 |
| 4 | 10.5—11.5 | 10.5—11.5 | 1.41 |
| 5 | channel 4 | 11.5—12.5 | 1.3 |

Source: Kidwell (1985).

The instantaneous field of view (IFOV) of each sensor is approximately 1.4 milliradians (mrd) leading to a resolution at the satellite subpoint of 1.1 km for a nominal altitude of 833 km. The maximum off-nadir ground resolution is 2.4 km along track and 6.9 km across track. The scanning rate of the AVHRR is 360 scans per minute.

The analog data output from the sensors is digitized on board the satellite at a rate of 39.936 samples per second per channel. Each sample step corresponds to an angle of scanner rotation of 0.95 mrd. A total of 2048 samples are obtained per channel per earth scan, which spans an angle of ca. 55.4° from the nadir (swath

width of 1600 km).

The infrared data are calibrated in-flight using a view of a stable blackbody and space as a reference. No in-flight visible data calibration is performed. Although these will vary from instrument to instrument, the design goals for the IR channels are a Noise Equivalent Temperature (NEdT) of 0.12°K (@ 300°K) and for a signal to noise ratio of 3:1 (0.5% albedo).

The AVHRR data are digitized to 10-bit precision. The digitized data are both transmitted from the satellite in real time (High Resolution Picture Transmission or HRPT data), and selectively recorded on board the satellite for subsequent playback as Local Area Coverage (LAC) data. A maximum of ten minutes of LAC data may be recorded per orbit.

The processor on board the satellite also samples the real time AVHRR data to produce reduced resolution Global Area Coverage (GAC) data. Four out of every five samples along the scan line are used to compute one average value, and the data from only every third scan line is processed. As a result, the spatial resolution of GAC data near the subpoint is actually 4.0 km by 3.3 km, although generally treated as 4 km resolution. All of the GAC data computed during a complete pass is recorded on board the satellite for transmission to earth on command. The 10-bit precision of the AVHRR is retained.

It can be generally assumed that areas within the window of HRPT coverage will have data available daily. LAC data, on the other hand, exhibits poor temporal resolution for most areas. For example, if a customer requires high resolution AVHRR data over Indonesia, on a date before the setting up of the LAPAN ground station in Jakarta, LAC coverage would have been scheduled for that specific area on that specific date.

**The TOVS data**

The TOVS complex includes three instruments:

1. The High Resolution IR Sounder (HIRS-2) is a 20-channel scanning radiometer with channels in the 4.3 $\mu$m and 15 $\mu$m regions and one visible channel. The IFOV of these channels are stepped across the satellite-track by use of a rotating mirror. This cross-track scan, combined with the satellite motion in orbit, provides coverage of a major portion of the earth. The width of the cross-track scan is 2240 km or 99° and consists of 56 steps. The optical IFOV is 1.25° which gives a ground IFOV of 17.4 km diameter at the nadir. At the end of the scan, the ground IFOV is 58.5 km cross-track by 29.9 km along-track; the Noise Equivalent Radiance (NER) ranges from 3 to 0.001 (miliwatts/$m^2$-steradians-$cm^{-1}$), according to the channels considered.

2. The Microwave Sounding Unit (MSU) is a passive scanning microwave spectrometer with four channels in the 5.5 mm oxygen region; which means

frequencies ranging from 50 GHz to 58 GHz with a channel bandwidth of 200 MHz in each case, and a typical NEdT of 0.3°K. The MSU sensors consist of two four-inch diameter antennas, each having an IFOV of 7.5° or 124 km: at the satellite subpoint there is an underlap of approximately 115 km between adjacent scan lines.

3. The Stratospheric Sounding Unit (SSU) is a step scanned IR spectrometer with three channels in the 15 micrometer carbon dioxide region. It makes use of the pressure modulation technique to measure radiation emitted from carbon dioxide at the top of the earth's atmosphere. The NER of the channels are respectively 0.35, 0.70 and 1.75. The SSU consists of a single primary telescope with a 10° IFOV which is step scanned perpendicular to the satellite subpoint track. Each scan line is composed of eight individual 4.0 second steps and requires a total of 32 seconds. The 10° IFOV gives a resolution of 147 km at the satellite subpoint and the stepping produces an underlap between adjacent scan lines of approximately 62 km at nadir. Every eight scans there is a calibration which is synchronized with the HIRS-2 instrument.

TOVS data are used for the derivation of atmospheric soundings, vertical profiles of temperature and humidity on a global basis, and to correct AVHRR data for atmospheric attenuation during the retrieval of sea surface temperature observations.

The useful routine products usually provided by the NOAA Center are described in the coming section dealing with the routine thematic NOAA products (p. 45).

## The NASA Satellites

Environmental data are or were provided also by several NASA satellites: HCMM, Seasat, Nimbus, etc.

The HCMM supported scientific investigations to determine the feasibility of using thermal IR temperature measurements of the earth's surface within a twelve hour interval, at times when the temperature variation was at maximum to determine thermal inertia. A mission duration of one year was planned. HCMM was launched on April 26, 1978, into a nearly sun-synchroneous 620 km circular orbit inclined 97.6 degrees (retrograde) to the equator. The HCMM orbit covered every area of the earth's surface between the latitudes of 85°N and 85°S at least once during the day (2 p.m. ascending node) and once during the night (2 a.m. descending node) within a 16-day interval. Both night and day passes over selected areas within a 12-hour period were repeated at 16-day intervals. The areas between 22° and 33° latitude (north and south) received only 36-hour coverage. All satellite operations ceased on September 30, 1980.

HCMM carried a two-channel scanning radiometer: 0.5 to 1.1 and 10.5 to 12.5 micrometers. The two channels thus provided measurements of reflected solar (NER of 0.2 mw/cm$^2$) and emitted thermal (NEdT of 0.4°K at 280°K) energy, respectively. From the nominal altitude of 620 km, the spatial resolution of the thermal infrared channel was 600 m at nadir, and the resolution in the reflectance channel was 500 m. The swath of data coverage along the track was approximately 716 km wide. HCMM data were collected in real-time when the satellite was within reception range of NASA receiving stations.

Seasat has been the first dedicated ocean observing satellite. It was launched on June 28, 1978 into a circular (800 km) orbit. Although Seasat's power failed on October 10, 1978, the 104-day mission has revolutionized microwave satellite oceanography. Seasat carried a payload of five instruments:

1. An active backscatter scatterometer system, operating at a frequency of 13.9 GHz, produced earth location and time tagged backscatter coefficients, surface wind stresses, and surface wind vectors (with a 180 degrees directional ambiguity); swath-width of 1200 km with a 100 km grid basis.
2. An active radar altimeter (13.5 GHz) which produced earth location and time tagged satellite heights, significant wave heights and geoid information; accuracy of 10 cm every 18 km.
3. A scanning multichannel microwave radiometer measured dual-polarized radiation from the earth at frequencies of 6.6, 10.7, 18.21 and 37 GHz. It produced earth location and time tagged SST, surface wind stress, atmospheric water-vapor, liquid water content and precipitation rate; swath-width of 1000 km with a 25 km spatial resolution for ice-features and 125 km for SST.
4. A microwave synthetic aperture radar with a 20.5° look angle from the nadir direction, a frequency of 1.275 GHz, and a H polarization, produced 25 m resolution surface roughness imagery with a 100 km wide ground swath for selected areas.
5. A visible and infrared radiometer produced imagery for identification of cloud and geographic features, for the microwave data: spatial resolution of 7 km.

Time and earth location tagged snsor and geophysical data from the Seasat instruments are available in digital form; the synthetic aperture radar data ae available both in digital and image form.

The Nimbus series of satellites are dedicated to instrument development. Their design is based on the Landsat series. The last one, Nimbus-7 (launched in 1978), is the single most significant source of experimental data from earth orbit, relating to atmospheric and oceanic processes. It carries a payload of eight instruments which provide measurements on a large scale basis:

1. A five-sensor visible and thermic radiometer (CZCS = Coastal Zone Color Scan-

ner) produce the color and temperature of the oceans and measures chlorophyl concentration, sediment and pollutant content. The bands centered at 443 nm and 670 nm were chosen because they lie in a region where the absorption of chlorophyl-a is high. On the other hand, the bands at 520 and 550 nm were chosen because they are located in regions where upwelling radiance variations do not depend on chlorophyl-a concentration. The "10.5—12.5 μm" band is for SST measures. The sub-nadir CZCS is 800 m and the swath-width about 1630 km.

2. A four-sensor microwave radiometer (SMMR) provides the brightness temperatures from the atmosphere and surface of the earth; for sea-ice monitoring, climatology, etc.
3. A 22 sensor radiometer (from UV to thermal IR) measures the earth and solar fluxes; for weather modeling.
4. A pressure-modulated thermic radiometer provides gas (CO, NO, $H_2O$, $N_2O$, $CH_4$, $CO_2$, $O_3$) concentrations and temperature profiles in the stratosphere and mesosphere.
5. A one channel (1 micrometer) radiometer that views the sun through the atmosphere measures the aerosol extinction profiles.
6. An UV radiometer provides ozone profiles by measuring the incident and backscattered solar radiation.
7. A two channel (6.7 and 11 μm) scanning radiometer provides earth's surface and cloud-top temperatures, and atmospheric moisture.
8. A six-channel thermal radiometer (LIMS) measures temperature profiles and gas concentrations in the stratosphere; for the study of upper atmospheric chemistry, especially of the nitrogen compounds and their relation to the distribution of ozone.

From the early 1980s, and at least throughout the following decade, the Shuttle will be NASA's transportation system for access to space. It will play a vital role in the developmet of future remote sensors, the calibration of instruments on operational weather satellites, the direct monitoring of slowly changing earth/atmosphere parameters, and the special experiments which are impossible or impractical by other means.

Some other sources of information must be stressed. The Geosat satellites are launched by the US Navy and carry a Seasat-type altimeter to determine the marine geoid (mean topography of the ocean). They provide information on mesoscale fluctuations in ocean surface topography, surface wind speed and wave height. Selected data from the DMSP (Defence Meteorological Satellite Program) satellites can also be available. They carry visible, infrared and microwave radiometers.

## THE GEOSTATIONARY SATELLITES

### Introduction

Currently this type of meteorological satellite include two US satellites (GOES) at 75° and 135° West Longitude, a Japanese satellite (GMS) at 135° East Longitude, and a European satellite (Meteosat) at 0° longitude. These satellites (Table 3) operate in a high orbit above the Earth. Their motion is synchronised with the Earth's rotation so that they appear to remain stationary over a point along the Earth's equator and afford repeated looks at a fixed field of view. One coves about 25% of the Earth's surface, generally 50 degrees of latitude north and south of the equator and 50 degrees of longitude east and west of the satellite's position along the equator (subpoint). During normal operations, full disk visible and IR views are transmitted every 30 minutes. Views of limited areas are transmitted as frequently as every three minutes during severe weather periods.

TABLE 3. GEOSTATIONARY SATELLITES

| Satellite | Position | Launch date | Operational data |
|---|---|---|---|
| GOES-1 | 126°W | 10/6/75 | 1/8/76-3/15/80 |
| GOES-2 | 107°W | 6/16/77 | 8/15/77-9/15/80 |
| GMS-1 | 135°E | 7/14/77 | 77- -1/84- |
| Meteosat 1 | 0° | 11/77 | 11/23/77-11/79 |
| GOES-3 | 90°W | 6/15/78 | 7/13/78-3/5/81 |
| GOES-4 | 135°W | 9/9/80 | 3/5/81-6/1/83 |
| GOES-5 | 75°W | 5/15/81 | 7/9/81-7/30/84 |
| Meteosat 2 | 0° | 6/81 | 6/19/81- |
| GMS-2 | 135°E | 8/10/81 | 81-1/84 |
| GOES-6 | 135°W | 4/28/83 | 6/1/83- |

Source: Kidwell (1985).

The payload carried by the last and future GOES satellites (NASA satellites) is described hereafter.

## The VAS Data

GOES-4 and the present geostationary satellites, GOES-5 and GOES-6 as well as future satellites in the series, are equipped with the VAS (VISSR Atmospheric Sounder), the successor to the VISSR (Visible and Infrared Spin Scan Radiometer) flown aboard earlier satellites in the series and on GMS.

The VISSR was primarily designed for cloud cover imaging at 30 minute intervals and earth/cloud brightness temperature measurements. It is a two channel radiometer: (i) one band (0.55—0.70 $\mu$m) in the visible, with a spatial resolution of 0.9 km (Figure 1), (ii) one band (10.5—12.6 $\mu$m) in the thermal infrared, with a spatial resolution of 8 km and a temperature sensitivity of 0.4—1.4°K (Figure 2).

The VAS instrument retains the VISSR dual-band imaging function (8 bit precision). However, the infrared channel capabilities have been expanded using a more complex configuration together with selectable narrow-band filters (10 bits precision). The VAS has six infrared detectors, two of which have a ground resolution of 6.9 km (0.192 mrd) and are used primarily for imaging. Four detectors have a resolution of 13.8 km (0.384 mrd) and are used for sounding operation. The additional spectral bands are sensitive to the effects of the atmospheric constituents; which makes it possible to determine not only the surface and cloud top temperatures as in VISSR, but also the three dimensional structure of the atmospheric temperature and of the water-vapor distribution. In addition, the VAS includes 12 narrow band infrared filters mounted on a filter wheel that is rotated to select the channels to be active. These filters are centered at 14.73, 14.48, 14.25, 14.01, 13.33, 12.66, 11.17, 7.26, 6.73, 4.53, 4.44 and 3.95 $\mu$m.

There are three VAS operating modes: (i) the VISSR mode: the sensor operates in a normal cloud-mapping mode; (ii) the multispectral imaging mode which supplies the normal VISSR cloud-mapping function and also provides data in any two additional spectral bands selected, with spatial resolution of 13.8 km; (iii) the Dwell Sounding mode, for which there is repeated coverage of a smaller area by more IR channels. It is performed to improve the data "signal to noise" ratio sufficiently to support derivation of vertical profiles of atmospheric temperature and humidity. This mode takes advantage of the use of the filters. Either the 13.8 km or 6.9 km resolution detectors can be selected.

World spread ground stations can receive VISSR data in real time. According to the level of the station, these data are VAS or only VISSR. The data may be later geometrically corrected. Several configurations are possible. So, in Indonesia the LAPAN (The Indonesian National Institute for Aeronautics and Space) ground-station receives only VISSR data with some time delay: the data are first transmitted from the GMS satellite to a Japanese station for processing:

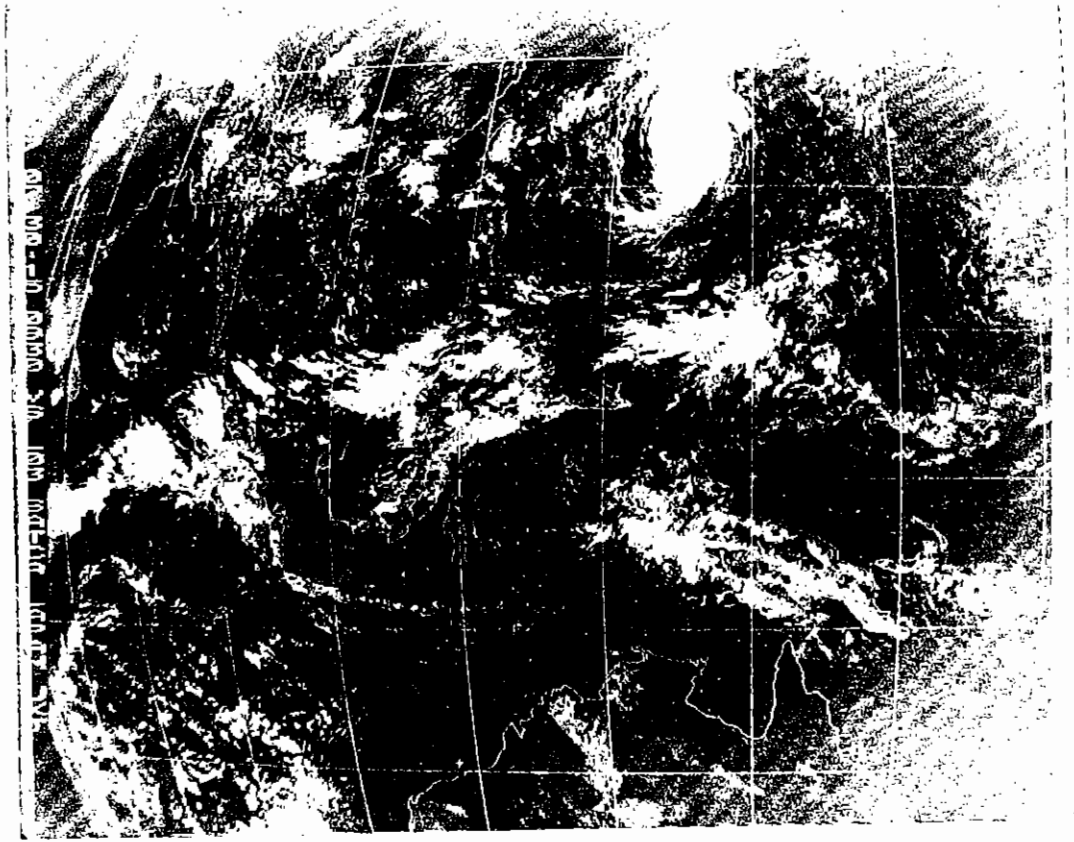

*Figure 1. GMS Visible Imagery**

Note:
* Collected by the LAPAN Station in Jakarta, at 07:30:15 GMT, the 10/07/82.

*Figure 2. GMS Thermal Infrared Imagery**

Note:

* Collected b the LAPAN Station in Jakarta, at 08:11:34 GMT the 10/07/82. It is displayed like a Mercator projection without atmospheric correction.

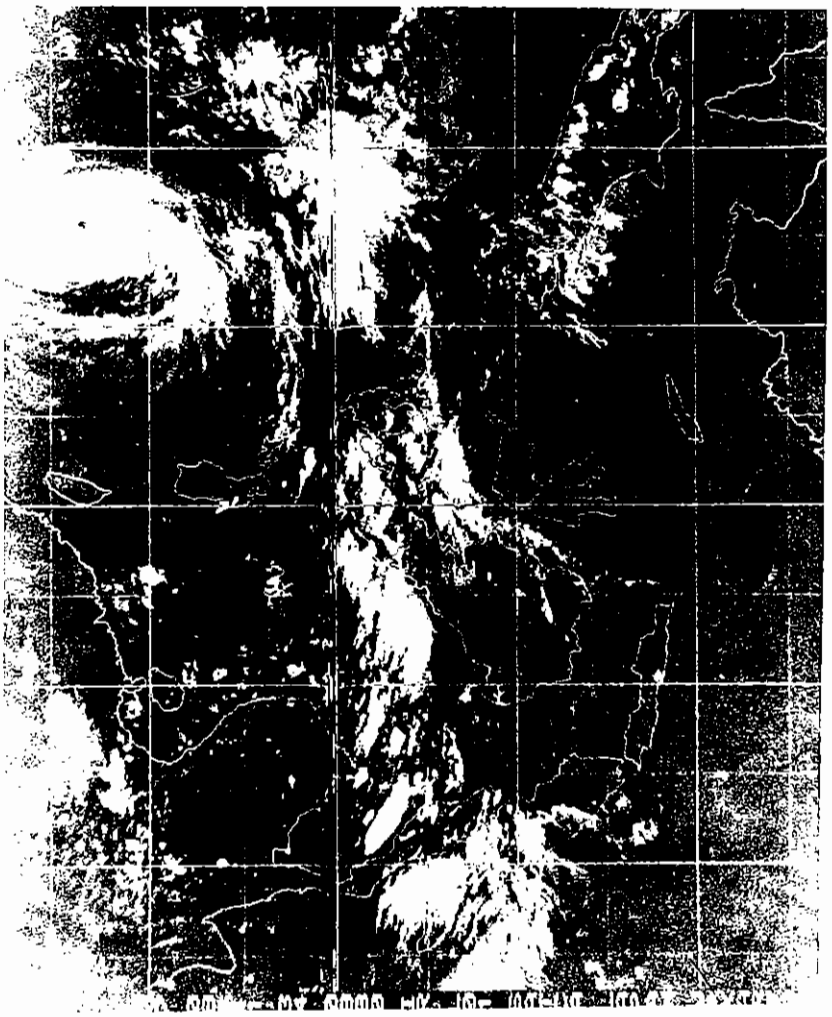

geometrical corrections, etc. In a second step these data are sent back to GMS from which they are transmitted to the LAPAN station.

In a general way, these data can be provided as digital or analog products with different preprocessing levels and geometrical configurations. The data available from the NOAA Center consist of preprocessed rather than raw data values. Visible data have been normalized and data from the IR channels have been adjusted to allow their conversion to tempertures by means of a standard table. The data are accompanied by orbit and attitude parameters that can be used to compute earth location information. Only limited quantities of VAS multichannel IR data are available from the NOAA Center. The usual routine products delivered by the NOAA Center are described in the following section.

## THE ROUTINE THEMATIC NOAA PRODUCTS

A rough description of the thematic products delivered by the NOAA Center is given hereafter. Their main interest is due to their daily and worldwide availability as digital or analog products.

They can be provided as raw data, from different satellites such as GOES or NOAA, with different geometrical configurations, i.e.: hemispheric polar-stereographic mosaics, Mercator mosaics, stretched gridded AVHRR strips. The latest one, for example, provide users with a "quick-look" and a view of the scene in the perspective and resolution of the original signals. The data in the visible part of the spectrum are used for general meteorological applications, i.e.: cloud coverage, cloud types, pattern of cloudiness, etc. On the other hand, the night time IR data are used to determine the approximate temperatures of the emitting surfaces. From these, the type of surface observed can be distinguished, and the heights of the cloud tops can be estimated.

The radiometrically processed data are also available. So, it is with the "seven day minimal brightness composite" of which the aim is to minimize the effects of cloudiness in satellite acquired AVHRR data over polar regions. By saving only the minimum brightness responses for a selected number of days, chart preparers can remove from that data set any relatively bright feature (clouds) that does not remain at the same location for the seven day period.

### The Meteorological Products

**1. Cloud-motion vectors**

They are computed with the help of geostationary satellites (GOES) data with a high time repetitivity (30 minutes).

**2. Atmospheric soundings**

The raw radiance retrievals of the three TOVS's atmospheric sounders, from the NOAA satellites, are converted into operational products consisting of the layer means temperatures (ca. 3°K) for standard pressure levels (850 mb), and of the layer precipitable water amounts (+30%) for three atmospheric layers. These data are archieved for input into current day products: global SST, weather analysis, etc.

**3. Global heat budget**

Visible and IR radiances, derived from averaging a 10 by 10 array of GAC (NOAA) data are combined with time, Earth location and angular measurements of satellite and sun altitude. The heat budget parameters are then derived, daytime and night time of longwave flux from 12 hours of IR retrievals. The absorbed solar radiation is computed from the difference between the solar constant and the visible spectrum retrievals. These data are mapped into 2.5° arrays by correcting for viewing angle and Earth curvature. The energy flow accuracy is ca. 7 $W/m^2$ and the spatial resolution is about 100 km. This product is of importance to long range forecasting and climate research.

**4. Weather summary and bulletins**

This is a general synopsis of the weather affecting the USA, which is supplied two to eight times per day.

**5. Cloud top temperature and tropopause height**

These data are provided from interactive man-computer retrieval of current IR digital data received from the GOES satellites. The accuracies are ca. 1°K and ca. 25 mb.

**6. Tropical disturbance summary**

This is a coded message listing all Satellite Weather Bulletins sent during the previous 24 hours and the locations of all vortices with tropical history, significantly disturbed areas and the intertropical convergence zone. The summaries are prepared by meteorologists using visible and IR satellite imagery from both the polar and geostationary orbiting satellites. This product is used by non-US weather operations in order to watch significant tropical weather conditions.

## Oceanic products

**1. The sea surface temperature (SST) products**

Global SST observations are acquired daily from the polar-orbiting

satellites' AVHRR sensor in the IR spectrum and from its high resolution IR radiation sounder HIRS. The model used in obtaining these SST is the MCSST (Multichannel SST). The SST observations are derived by a maximum likehood technique applied to 50 km resolution target arrays of GAC (4 km resolution) data. Acceptable SST targets are determined by a comparison with coincident equivalent brightness tempertures derived from HIRS data revealing a cloud-free target. The accuracy goals are ca. 1.5°K: for the relative precision it is ca. 0.5°K. These goals are achieved over approximately 70% of the global ocean. The derived observations are stored for immediate or future utilisation.

The routine multichannel-algorithm (McClain, 1982) for the atmospheric correction of the NOAA day-time data uses the two radiance temperatures, T' and T", corresponding to the two IR channels centered around 11 mm and 12 mm. The processed temperature is given by:

$$T = 1.0351\ T' + 3.066\ (T'-T") - 283.93$$

Some users who perform atmospheric corrections of AVHRR data use, when they are available, some simultaneous in-situ data as calibration points. This method which is rather easy is not necessarily less accurate. Another process consists in modeling the atmospheric effects. This method requires the knowledge of numerous physical parameters. One of its main constraints is due to the non-horizontal homogeneity of the atmospheric layers (Callison and Cracknell, 1984).

**The Oceanographic Analysis Charts.** Their purpose is to delineate the position of the cyclonic and anti-cyclonic Gulf Stream surface frontal zone, the location of Gulf Stream meanders, filaments and eddies, and the identification of the various water masses based on temperature. The daily products are relative to the areas limited by 35°N—50°N / 44°W—76°W and 19°N—32°N / 65°W—97°W.

**The MCSST 1° Global Contour Charts.** Isotherms with a 100 km spatial resolution which are plotted on sets of SST 1° charts. The coverage is limited to 70°N—70°S with 24 charts (Figure 3). Although 1° SST data are available daily, these charts are generated once a week; the bulk of the data being from the day before the date of generation.

**The MCSST 0.5° Regional Contour Charts.** These 0.5° charts are produced for three separate regions: the US Atlantic coast, the US Pacific coast, and the Pacific Ocean around and between Alaska and Hawaii. Isotherms of 1°K are drawn with a spatial resolution of 50 km.

**The MCSST Monthly Mean Contour Charts.** At the end of each month all the satellite observatons are averaged and plotted on 2.5° by 2.5° grid: 1°K isotherms with a 250 km resolution for six 75 latitude (65°N—10°S

or 10°N—65°S) by 130 longitude areas.

**The Digital Products.** Daily computations of SST values at each 1° longitude/latitude are stored on CCT. Lower resolution global SST gridded data set (5°) is generated by averaging the 1° data set. Monthly mean SST gridded (2.5° by 2.5°) data are also routinely computed and stored.

**2. The ice charts**

**The Great Lakes Ice Analysis.** It is a description of ice-conditions (extent of ice, ice-fast areas, etc.) in the sea-ways of the North American Great Lakes, with the help of AVHRR LAC and GOES VISSR imagery, in the absence of clouds. It permits the forecasting of the limits of the shipping season and the routing of commercial shipping. The accuracy of positioning is within ca. 5 km.

**The Polar Regional Ice Charts.** The information is provided with the help of the three satellites NOAA (AVHRR), DMSP and Nimbus (ESMR). These charts cover Arctic and Antarctic areas. The accuracy of ice-limit positioning is ca. 5 km.

**3. The ocean current analysis**

**The Gulf Stream Wall Bulletin and Analysis.** The human anlysis of NOAA (AVHRR) and GOES (VISSR) imagery leads to a description of the western boundary of the Gulf Stream (accuracy ca. 5 km). It consists of plotting current position, areas of cold and warm eddies, etc. to help the mariner in locating areas of good fishing and reducing cost in transporting merchandise.

**The West Coast Terminal Front Analysis.** The waters off the US west coast are analysed with AVHRR rectified 1 km data. An estimated accuracy of +5 km is achieved in the locations of frontal zones.

**The Hydrological Products**

**1. The river basin snow coverage observations**

For selected river-basins, the analysis of cloud-free NOAA (AVHRR) and GOES (VISSR) imagery leads to run-off forecasting, flood prevention, water resource-planning, irrigation, etc. This product is accurate to 5% in areas larger than 5000 sq. km.

*Figure 3. GOSSTCOMP Sea Surface Temperature the 1/03/84*

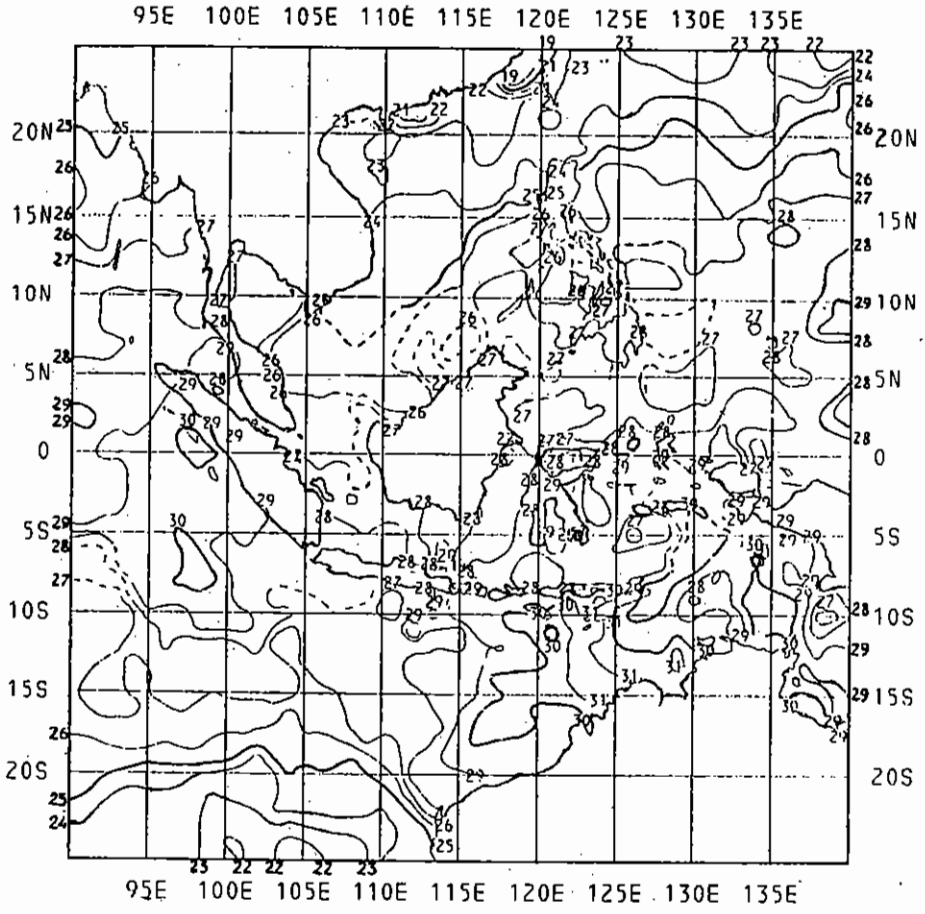

2. **The regional snow cover analysis**

The snow boundary positioning (ca. 5 km) is usually mapped for the Great Lakes, North Eastern USA and the Himalayas, with spatial resolutions of 1 km (GOES) and 4 km (GAC) data.

3. **The northern hemisphere snow and ice chart**

It consists of a weekly snow and ice coverage of the northern hemisphere. For areas where several observatiosn are made, and accuracy of ca. 50 km can be achieved.

### The Vegetation Products

The NOAA global vegetation index has been produced since 1982. It is based on the resampling of the worldwide GAC (4 km resolution) to a 15 km resolution grid. To minimize atmospheric interference and sun-angle effects, the data are maximized weekly and a weekly Green Vegetation Index (GVI) is produced. This product is highly reliable in terms of temporal coverage. Quite better spatial resolutions can be achieved by users with the LAC data. An example of the use of this product is given later.

## APPLICATIONS

Some applications for a maritime tropical country, such as Indonesia are for crop, disaster and fishery monitoring.

### Agroecosystem Monitoring

Assessing agroecosystem productivity and sustainability is conditioned by the ability to measure relevant parameters at repetitive intervals. In complex and diverse systems associated with tropical agriculture, monitoring is a difficult task. For example, individual crop observations are traditionally performed on a sampling base by a large number of agricultural agents dispersed throughout the country, so that the aggregation time is very long.

For agroecosystem monitoring, it is very important to measure the dry matter content of the present vegetation. Total above ground dry matter production or the net above ground quantity of dry plant material per unit area produced per unit of time via photosynthesis is a measure of primary ecological importance. This biological quantity is largely determined by abiotic conditions and climate in particular. It represents a means for quantifying the net photosynthetic activity

within regions and/or between years. As such, the ability to measure total dry matter production or a closely correlated parameter over large areas is of great utility to ecologists, climatologists, and natural resource managers.

Satellite Remote Sensing offers the potential to survey larger than 10,000 km areas in an economical fashion. The remote sensing technique which is now widely used involves linear or ratio combinations of a spectral channel in the 0.6—0.7 μm and 0.75—1.1 μm regions. Radiances in the red region are inversely related to the in-situ chlorophyl density, while radiances in the near IR are directly related to the projected leaf area index. The use of red and near IR data is based upon the ability to spectrally estimate the photosynthetically active biomass (green leaf area) and upon the relationship of the intensity and duration of the photosynthetically active biomass through time to the total dry matter production (Markham *et al.*, 1981; Tucker *et al.*, 1981). Ratio and linear combinations of red and photographic IR spectral data have been used in different vegetational situations including tropical forests, grasslands and agricultural crops.

In general it appears that data collection at intervals of 5—14 days is needed to adequately estimate the temporally dynamic nature of the photosynthetically active biomass. The 18-day Landsat repeat cycle is thus not suitable; moreover due to the nebulosity constraint the effective repetitivity of 18 days is not sufficient. The previous statements lead one to consider that the AVHRR data as a very good tool for vegetation monitoring because of its low price, large coverage, and high repetitivity.

It must be stressed that the extraction of precise information requires the inclusion of additional data on farming practices, crop calendars, topography, soils, etc. Generally this approach requires analysts who are familiar with the region, or having at least access to computer compatible data relevant to the locality. With the development of the microcomputer industry, such an approach becomes a reality. Moreover it becomes also possible to combine different remote sensing data, such as high spatial resolution visible data with low spatial resolution thermal IR data.

Two examples of temporal linear combination ratio are given in Figures 4 and 5. They have been derived from data sets contained in the NOAA Global Vegetation Index. One is taken over a rice growing area of Java (Indonesia) and the other over a wheat-rice growing area of the People's Republic of China. One could a priori assume that data of such coarse resolution are totally inappropriate for observing the traditional rice landscape of Indonesia or China. Yet, as the attached figures show, seasonality changes in crop biomass are well displayed. For Java, the dry and the wet season rice crops are well differentiated; peaks (full cover) and lows (fallows) are well marked. The 1982 drought is reflected by the lower values of the vegetation index for the dry season crop and by the delay of the planting of the

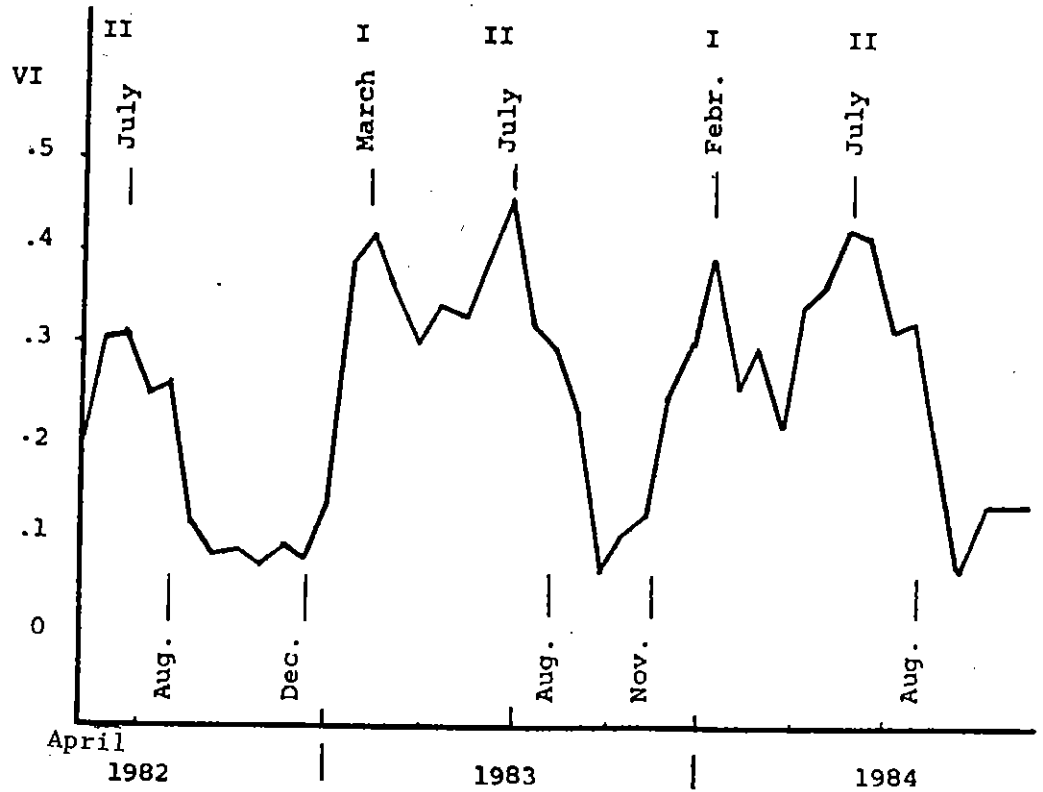


*Figure 4. 1982—194 Vegetaion Index for an Irrigated Sawah Area (rice fields) on the Northern Coastal Plain of Java*

Note:
The wet (I) and dry (II) seasons are well differentiated. The impact of the 1982 drought is evidenced by the Low Vegetation Index values for the dry season crop and the long fallow period.

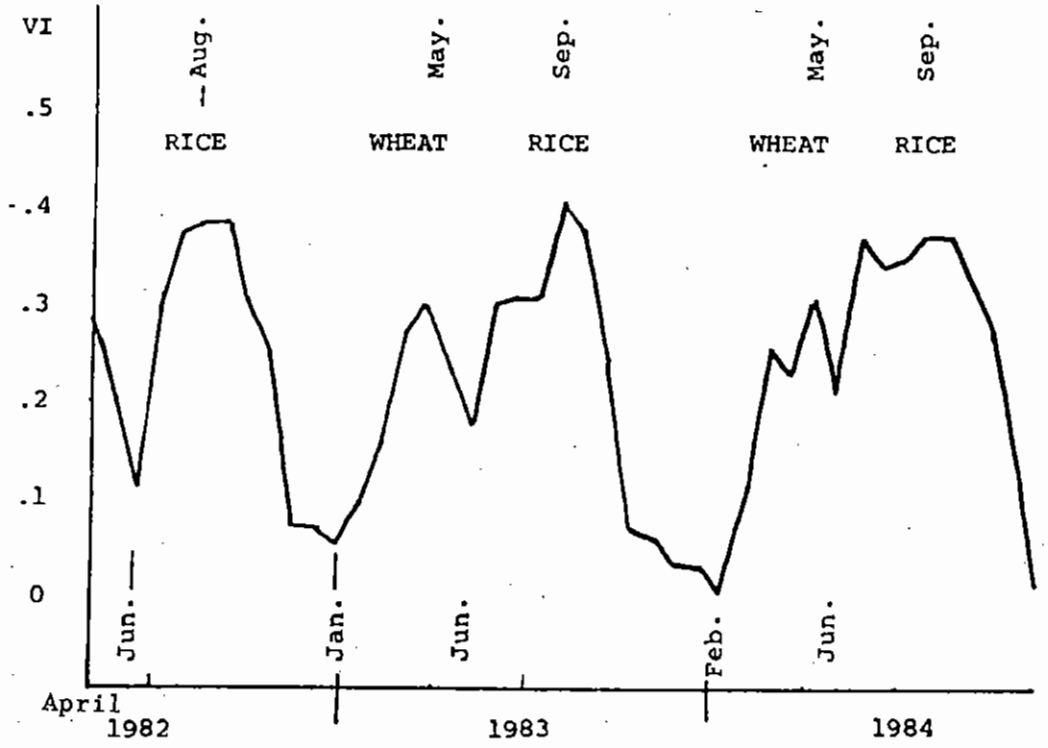


*Figure 5. 1982—1984 Vegetaion Index (VI) for the Taizhou Area in Jiangsu Province*

Note:
At the exception of the 1984 crops, due to a delay in wheat growth, the winter wheat and summer rice crops are well distinguished with lower "VI" values for wheat than for rice. Data from Global "VI" 15 km resolution data.

following crop (compare with the 1983 and 1984 situations). For China, the winter wheat and summer rice are easily differentiated. Dates of planting and harvesting are clear and correspond to the dates provided by the local agricultural sevices.

One can immediately foresee the possible uses of such temporal plots. They provide a unique set of data for monitoring agricultural activities and crop conditions. They can be used to confirm agrometeorological models of crop development and for early warning in case of impending crop failure. The operational use of the vegetation index approach presupposes, however, that a framework exists for interpreting such information in terms of "normal" or "abnormal" behaviour for the crop under observation. In this respect, much remains to be done to characterize the vegetation index temporal changes better and to relate their characteristics to crop growing conditions in the agroecosystems.

Continent-wide classification and monitoring of vegetation is possible with the AVHRR data. Indeed, the temporal compositing approach, in which the maximum value of the vegetation index is kept throughout a period of time, is an efficient means to overcome the problem of extensive cloud cover. Once cloud-free data are available at frequent intervals, the large-scale dynamics of the green leaf biomass can be recorded. Seasonal variations of the vegetation index can be analyzed not only for selected pixels as illustrated in the preceding section, but for entire ecosystems or agroclimatic zones. The pulse beat of the whole biosphere can thus be recorded. While such specific application may be of less direct relevance for local development objectives, it may provide a useful framework for analysis. Indeed, it is increasingly recognized that there are connections between the different parts of the biosphere and that local actions can have global repercussions (the Kalimantan forest fires). Global observation tools have, therefore, a logical role to play in the panoply of instruments designed for studying biotic processes.

### Disaster Assitance and Crop Forecasting

In 1982—1983, climatic anomalies lead to severe drought in several countries of the western rim of the Pacific Basin. Agricultural production was affected in parts of the Philippines, Indonesia and Papua New Guinea. The tropical forest of East Kalimantan was also affected. An important tree mortality and the accumulation of litter provided appropriate fuel for the spreading of fires which, by the year 1983, damaged more than 3 million hectares. The extent of the disaster was completely unsuspected until the end of the year 1983, when the first aerial surveys were conducted. Could remote sensing data help to forecast the magnitude of such a disaster? Was it possible to estimate easily and quickly the extent of the disaster? The answers are fully positive.

Due to its high temporal repetitivity, NOAA-7 provided 15 relatively cloud free scenes of the whole island of Kalimantan since February to October 1983. By comparison, Landsat yielded only 2 cloud free images of East Kalimantan during this period. An intensive analysis of the AVHRR archives (GAC data) has shown the appearance of anomalies related to the degradation of the forest ecosystem, i.e.:

(i) in 1982, NOAA data permitted to detect the first signs of an El Nino in the Southern Pacific where sea surface temperatures were abnormally high. It was possible to designate, with a more or less good accuracy, which areas (South America, Carribean, Southern Africa, South and Southeast Asia) would be affected.

(ii) a gradual decrease in the vegetation index of the forest canopy of East Kalimantan for months before the forest fire occurred, reflecting trees conditions in the vegetation (Figure 6).

(iii) the appearance of a growing number of "hot points" in early 1983, related to the increased land clearing activities and to the rapid extension of the fire as the drought intensified it. Most of the fire was doused by the heavy rains of May 1983. In order to detect it, a fire does not need to have the size of the 4 km AVHRR data. At fire temperatures (300—600 C), the emitted radiant energy is higher in the "3.6 m" channel than in the 11 m (Figure 7).

(iv) the appearance in April of an enormous mass of smoke lingering for several months over the island. It extended to Singapore and Peninsular Malaysia more than 1500 km to the west.

On the remotely sensed imagery the damages to the vegetation are displayed by a slight increase in the visible channel and a drastic decrease in the near IR channel (Malingreau, 1984). By contouring the burned area of East Kalimantan, it can be estimated that about 3.1 million hectares were affected at various degrees of severity.

It is sure that the knowledge in "real-time" of these informations could have permitted the authorities, in a first step to reduce the magnitude of this disaster, and in a second step to improve the situation more quickly.

The monitoring of volcanic explosions with environmental satellites is also valuable. The explosion of the Galunggung (Indonesia) in April 1982 was observed with the NOAA and GMS satellites (Figure 8). Ash plumes produced by active volcanoes are best identified in the visible and near IR channels where the "water vapor-ash" mixture highly reflects the solar radiation. The reflectivity of these plumes decreases with the distance because of the reduction in water vapor and in aerosol concentrations, due to dispersion and scavenging. At very low density levels, the ash shows a diffuse grayish tone. Sequences of images are thus often necessary to monitor the travel and to separate, with some degree of certainty.

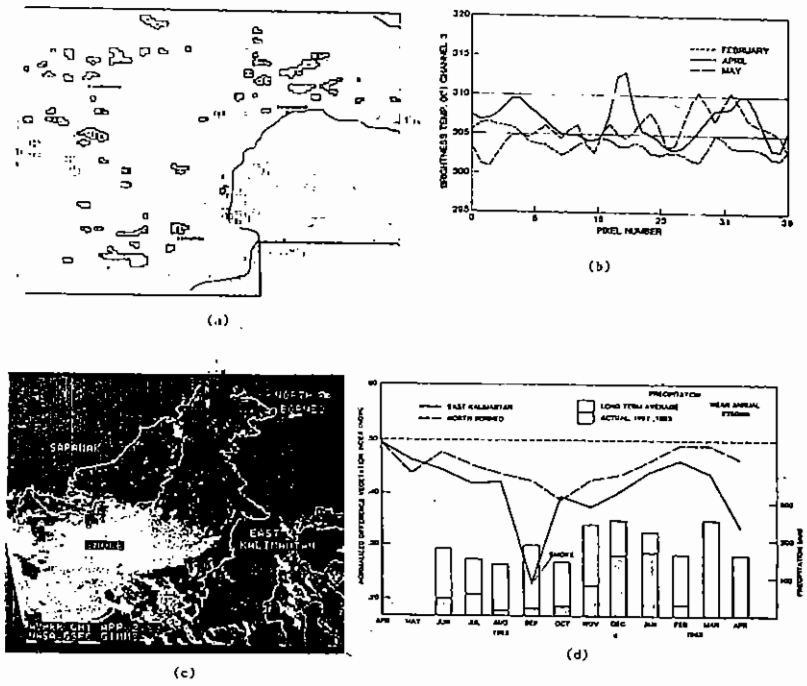


*Figure 6. (a) Computer printout showing the location of large forest fires in East Kalimantan as seen on April 2, 1983 by the NOAA-7 AVHRR thermal channel 3; the brightness temperature interval is 310—320 K.*
*(b) Local AVHRR channel 3 (GAC data) transect in North East Kalimantan showing the normal pre-fire pixels of February, the peak fire pixels of April and the remaining hot spots of May.*
*(c) The extensive smoke cloud created by the forest fires of April 1983, in East Kalimantan are easily distinguished on this AVHRR visible channel image.*
*(d) 1982—1983 changes in the Vegetation Index of the tropical forest of East Kalimantan and North Borneo (AVHRR data).*

*Figure 7. Display of Kalimantan with Channel 2 AVHRR Data, on March 1984, after the Forest Fires.*

Note:
The clouds are represented by the white tone (white and pink colors).

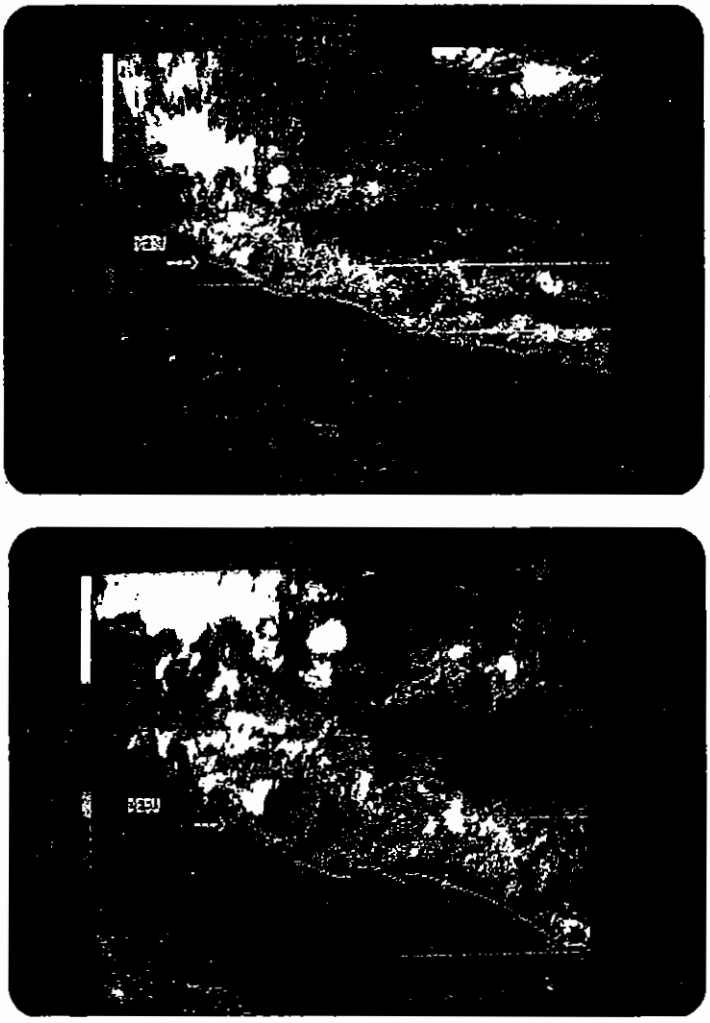

*Figure 8. Explosion of the Galunggung Volcano (Java, Indonesia).*

Note:

The upper layers of the ashes, mixed with clouds, are cold and highly reflexive (white and red) whereas hot dust is displayed in dark tone (blue color). These channel 2 AVHRR data from NOAA-7 were received by LAPAN, on 3 June, 1982, 2 p.m.

the ash plume from other atmospheric features. The rise of the eruption cloud can be monitored by the thermal AVHRR channels with the help of air temperature profiles. Indeed the estimate of the temperature of the outermost layer of the rising column, which equals to the surrounding air temperature, allows its altitude to be determined.

The NOAA currently provides a Disaster Early Warning Programme based on weekly rainfall/weather analysis and climatic impact assessment models for more than 350 agroclimatic regions. This programme is largely based on monthly rainfall data because rainfall is the primary meteorological element which determines year-to-year variations in yield. The variance of monthly and seasonal rainfall is 500—1000 times larger than the one of other meteorological elements. Regional rainfall estimates are determined with ground station reports; their accuracy being improved with the satellite cloud data.

With the help of remotely sensed vegetation condition (vegetation index) weather data are then interpreted by regional agroclimatic indices (soil moisture, plant water deficit, etc.) which indicate potential crop production in relative terms. These indices are compared to the historical occurrences of crop failure, food shortages, drought, flooding etc. Finally, climatic impact and the potential for abnormal food shortages are identified from these indices. Crop models can provide more tailored information (phenology forecasting with plant process models) than indexes, but they require more resources to build and operate. Consequently it appears that agro-climatic/crop index models based on simple cumulative rainfall over the crop season are vastly superior to most statistical/climate crop yield models based on linear correlation and regression analysis. Agro-climatic assessments works best for rain-fed agriculture, whereas drought is much more reliably assessed than flooding. It must be pointed out that microcomputers (such as the Apple II) are quite useful in order to manipulate this type of data base.

In South and Southeast Asia, NOAA uses two types of agro-climatic/crop condition indices. Both indices require 20—30 years of historical monthly rainfall data which are used to interpret current index values in terms of past values. The first is a monsoon index, usually June—September for the southeast monsoon and October—January for the northeast monsoon in the northeast latitudes with adjustments for Indonesia. The second index is for specific crops and is calculated according to crop calendars and crop water requirements.

In Indonesia the assessment of climate impact on agriculture is produced by the Climate Impact Assessment Service which is a joint effort of the Meteorological and Geophysical Agency, Directorate General of Food Crop Production, National Logistics Agency, and the Central Bureau of Statistics. The reports summarize the significant weather events and their impact on agriculture in various parts of the country. The information is presented as tables (weather

induced agricultural damages by province), maps (actual and long term mean decade rainfall for Madura and other islands: damaging weather which occurred until the present 10-day period at delineated areas) and graphs (historical records of rainfall, soil moisture and evaporation: actual and decade cumulative per cent area harvested since January). Several types of indices are used such as the Generalized Moisture Index, the Current Yield Moisture Index, etc.

## Fishery Monitoring

Fishery assessment and productivity may be assisted by measurement of aqueous parameters which affect fish distribution. The common approach is to investigate the relationship between a certain fish stock and a single remotely measured parameter. The possible parameters include temperature (thermal IR and microwave), salinity (microwave), chlorophyl (visible), turbidity (short visible), and sea-state (passive and active microwaves). Actual accuracy of techniques for remote measurement of salinity using microwave is of the order of 1%, which can only be useful for estuarine and nearshore fisheries. The parameters "turbidity" and "sea-state" cannot be remotely measured with a sufficient accuracy for fishery uses.

Typically, the concentration of chlorophyl—a is used as an indication of phytoplankton biomass because of the ease with which this quantity can be measured fluorometrically. However, with multispectral imagery, the index of phytoplankton biomass is provided by the sum of the near-surface concentrations of chlorophyl-a and of pheopigments (pigments). At the pigment concentrations usually encountered, it should make no appreciable difference if one uses the chlorophyl concentration or the pigment concentration, since the pheopigment concentration is only 10% or less of the chlorophyl concentration: which is well below the inherent error in the usual satellite-derived estimate of the pigment concentration. One determines pigment concentration by measuring the radiance diffusely reflected from the ocean in the blue and green spectral regions. .Accurate results can be achieved only with the use of sensors with narrow spectral bands. Water with low phytoplankton pigments reflects more blue light than green, whereas water with high pigments reflects more green light as a result of the selective absorption of blue light by the pigments. Before the pigment concentration can be estimated, one must remove the radiance due to backscattering of the sun radiation by the atmosphere. The chlorophyl concentration can be used as a general index of primary (carbon) productivity on a regional scale (Smith and Bake, 1982). At this time, mainly due to the complex interaction of scattering and absorbing effects by the different constituents (suspended sediment, yellow substances, etc.) within sea-water, the errors on the chlorophyl satellite measures

are too large (as far as 50%) to allow a sytematically reliable information about the fish spatial distribution. Nevertheless satellite-derived ocean colour charts are produced by NASA, with CZCS data, in support of commercial fisheries (Montgomery, 1981). With these charts (Figure 9), fishermen are able to locate particular species of fish in particular colours of water, since the colour is strongly related to the origin, temperature and nutrient levels of the water masses.

While colour acts as an indicator for some fish species, for others the temperature range is vital. In fact, the water surface temperature is the easiest parameter to measure if it is tolerable to restrict the observation to a few microns of depth (Gastellu-Etchegorry *et al.*, 1983). It is also the most effective technique. Indeed, it has been long known that some oceanic thermic structures, mainly the oceanic fronts, favour the concentration of fishes (tuna-like fishes). In fact the emphasis must be laid more on the thermic gradients than on the absolute accuracies of the measures.

Throughout the world, plenty of fishermen take advantage of the remotely measured sea surface temperatures. With the improvement of the technology (improved accuracy and repetitivity) such a tendancy is due to increase. So, in Indonesia an experiment is nowaday taking place in order to show the usefulness of remote sensing for local fishery. In-situ SST, salinity, and fish productivity are obtained by the BPPL (Indonesian Oceanographic Center)/ORSTOM (French Research Center), whereas simultaneous AVHRR data, received at the LAPAN ground station, are analysed in the Laboratory of Remote Sensing (PUSPICS) of the Gadjah Mada University Yogyakarta. It is intended to establish correlations between the fish productivity and isotherms (Figures 10 and 11). Such an experiment would have to be continued in order to lead to daily routine temperature charts, similar to the NOAA's MCSST but adapted to Indonesia. Such an approach, if continued and generalised, will surely have an important economic impact.

## CONCLUSION

The emphasis has been laid on the use of some relatively new instruments for resource inventories and environmental monitoring. Global monitoring tools such as the NOAA-AVHRR provide a new perspective on resource distribution and dynamics. Due to their coarse ground resolution and their high temporal resolution, the interpretation of such data must focus on temporal changes at a higher level of spatial aggregation than with the other remote sensing data (Landsat, SPOT).

The meteorological satellite data are used more and more for monitoring

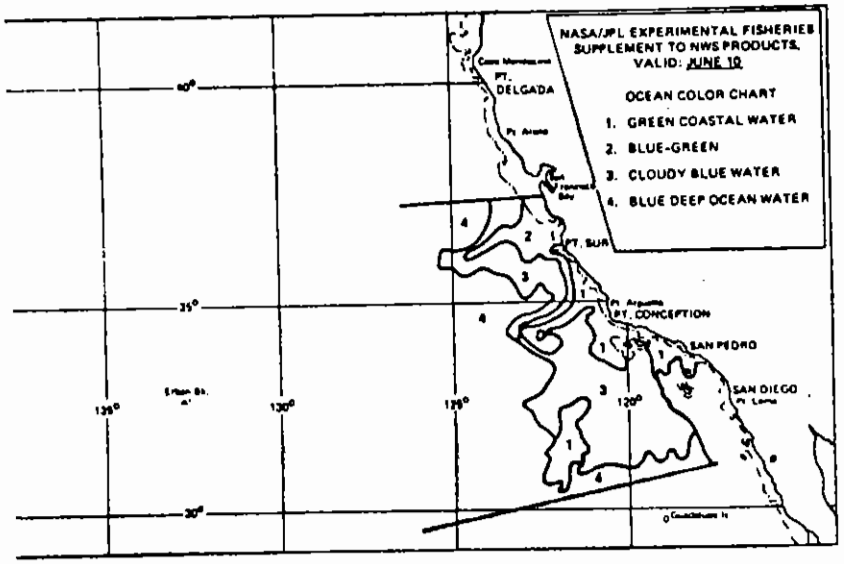


*Figure 9. A Satellite-derived Ocean-colour Chart Produced to Assist Commercial Fisheries off California* (from Montgomery, 1981).

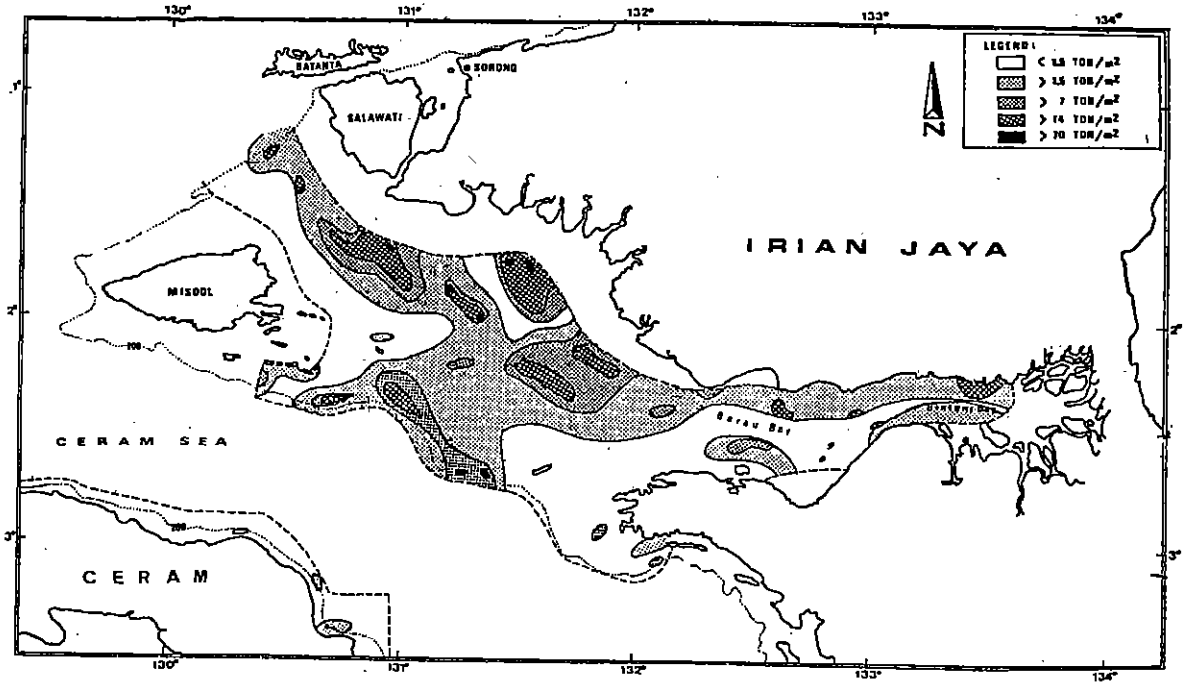


*Figure 10. Distribution of the Fish Densities (tons/square mile) Aside Irian Jaya.*

Note:
Estimated with in-situ measurements during the Corindon mission (Boely *et al.*, 1984).

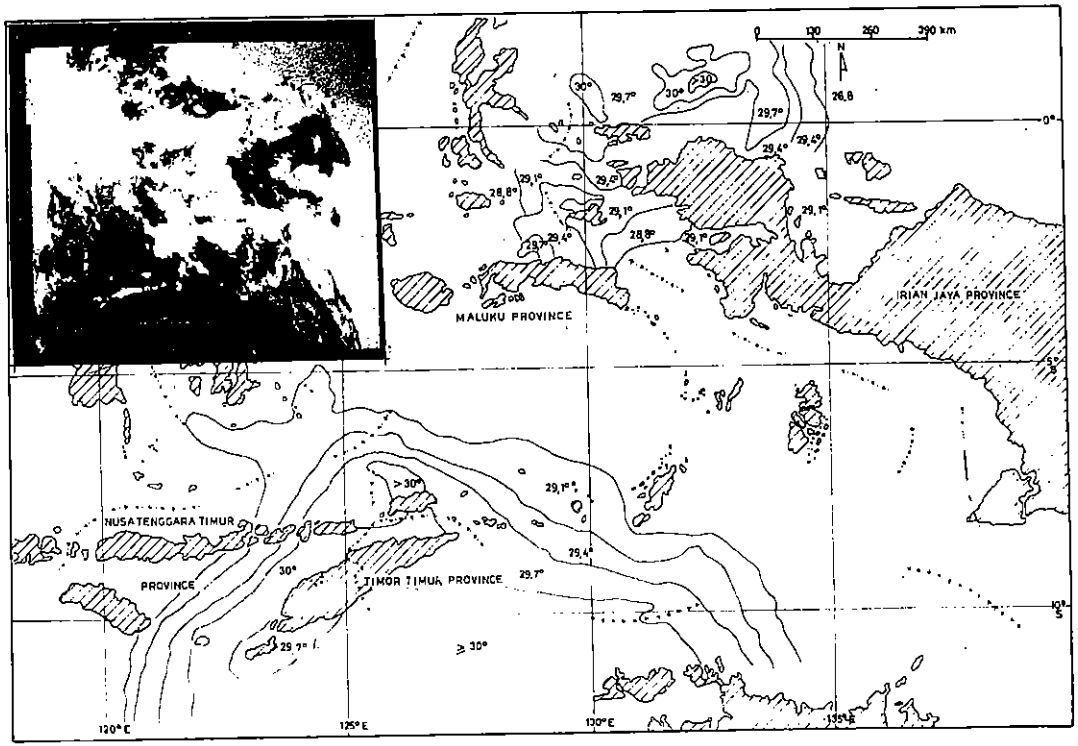


*Figure 11. Isotherms Derived from Channel 4 AVHRR Data* *

Note:

* Collected at LAPAN during the Corindon mission. Even the high repetitive NOAA data, due to a persistant cloud cover, did not allow a good daily monitoring. The GMS data allow it but the SST accuracy is too low (more than 0.5° K).

the inter-relationships between the atmosphere, the oceans and the land. They are also useful for forestry, agriculture, drought, watershed and fishery assessments. When used as part of a Geographic Information System they reduce the cost and improve the accuracy of operational crop, drought, fire and assessment programmes. It must be stressed that in order to get a useful product, it has to be possible to compare the analyzed temporal changes with reference data. That is the case for the evaluation of the vegetation and the sea surface temperature. For crops, the use of a continuous monitor and complementary information, such as meteorological and agricultural data permits the forecasting of the size of the harvests and so that it helps the food security management. It is possible to detect drought and assess drought affected crop production losses as long as 30 to 60 days before harvesting, which represents a three to six months early warning before food shortages happen. Such an information can be used to avert or mitigate the consequences of drought.

In Southeast Asia, several stations, i.e.: Jakarta, Singapore, Kuala Lumpur and Bangkok receive NOAA and GMS data in real time. It will need little additional processing in order to develop a major source of information on important regional changes.

## REFERENCES

Boely, T. and Subhat Nurhakim. 1984. Results of the Cruises Corindon 10 and 11 in Ceram and Irian Jaya. Paper Presented at *The Franco-Indonesian Symposium for Oceanology*, Jakarta, 1984.

Callison, R.D. and Cracknell, A.P. 1984. Atmospheric Correction to AVHRR Brightness Temperatures for Waters around Great Britain. *International Journal of Remote Sensing*. 5(1): 185—199.

Gastellu-Etchegorry, J.P. and Pramono Mardio. 1983. The Remote Sensed Sea Surface Temperature: a Case Study in Indonesia. *The Indonesian Journal of Geography*. 13(46): 13—27.

Kidwell, K.B. 1985. *NOAA Polar Orbiter Satellites—Users Guide*. Environmental Information Summary C-16 of the National Oceanic and Atmospheric Administration.

Mac Clain, E.P. 1982. SST Processings. Unpublished document presented to *NOAA/NESS Sea Surface Temperature Research Panel*, at 32nd Meeting, Washington, 30 September 1982.

Malingreau, J.P. 1984. Remote Sensing and Disaster Monitoring: A Review of Applications in Indonesia. Paper presented at *The 18th International Symposium on Remote Sensing of the Environment*, Paris.

Markham, B.L., Kimes, C.J. Tucker, and McMurtrey J.E. 1981. Temporal Spectral Response of a Corn Canopy. *Photogrametric Engineering and Remote Sensing*. 48(11): 1599—1605.

Montgomery, D.R. 1981. Commercial Applications of Satellite Oceanography. *Oceanus*. 24: 56—64. Woods Hole Oceanographic Institution, Woods Hole, Mass.

Smith, R.C. and Baker, K.S. 1982. Oceanic Chlorophyl Concentration as Determined by Satellite (Nimbus-7 Coastal Zone Colour Scanner). *Marine Biology*. 66: 269—279.

Tucker, C.J., B.N. Holben, J.H. Elgin, and Mc Murtrey J.E. 1981. Remote Sensing of Total Dry-Matter Accumulation in Winter Wheat. *Remote Sensing Enviroment*. 11: 171—189.

## ANNEX

A simple energy argument shows that a satellite moving without friction in a gravitation field of a spherical planet has a trajectory which is either elliptical, parabolic or hyperbolic, depending on its starting velocity. For an Earth-orbiting satellite, an elliptical orbit is required.

The movement of an Earth orbiting satellite, in the absence of perturbations, is fully determined with the use of 6 parameters, i.e.: 2 parameters (i and $\Omega$) define the orbital plane relative to the stars, 1 parameter (w) fixes the ellipse orientation within the orbital plane, 2 parameters (e, a) characterize the shape and size of the ellipse, and 1 parameter ($\Theta$) defines the satellite's position within the ellipse:

- i : inclination of the orbital plane to the Earth's equatorial plane,
- $\Omega$ : right ascension of the ascending node, measured eastward from the point of Aries (fixed point in the heavens),
- w : angular distance of the perigee around the orbit, measured from the ascending node,
- e : eccentricity of the ellipse,
- a : semi-major axis of the ellipse,
- $\Theta$ : angular position of the satellite in its elliptical orbit.

For the elliptical orbit displayed below (Figure A), the distance "r" of the satellite from the center of the Earth is given by:

$$r = a\,(1 - e^2)/(1 + e.\cos(\Theta))$$

The satellite period "T" round the plane orbit defined with Newtonian dynamics is:

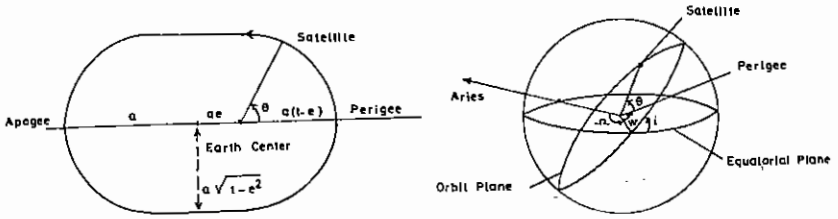


*Figure A. Satellite Elliptical Orbit*

$$T = 2\pi (a^3/G.M)^{1/2}$$

where "G" is the constant of gravitation and "M" the mass of the Earth. For a low orbiting satellite: a#R (Earth radius) and T#100 mn; for a geostationary satellite: T = 1 day and a = 42,290 km.

The angular speed relative to the Earth of the satellite on its plane orbit is given by:

$$d\Theta/dt = (G.M.a\ (1 - e^2))^{1/2}/r^2$$

In practice, disturbances must be considered. So, the drag of the atmosphere on low orbits results in the acceleration and eventual burn-up of satellites. However, during the operational life of the environmental satellites, this effect can be neglected; so can be the effect of solar wind and radiation, unless the satellite has a very low density and a large surface area. The principal deviation from a pure elliptical orbit is due to non-symmetrical gravity forces owing to the irregular figure and mass distribution of the Earth. Solar and lunar gravitation are quite less significant. It is shown that the equatorial bulge of the Earth causes a slight change to the period, and results in the perigee of an elliptical orbit changing position with time, that is, $dw/dt \neq 0$.

In order to get a sun-synchroneous orbit, the orbit plane must undergo one rotation per year: $d\Omega/dt = 0.986$ per day. In this way the orbit plane is not fixed relative to the stars but to the sun: the satellite crosses the equator at the same local solar time on each pass, throughout the year. This rotation is achieved with

the inclination of the orbit plane, owing to the precessional mechanism:

$$d\Omega/dt \propto - (G.M)^{1/2} .R^2 .a^{-7/2} (1 - e^2)^{-2} \cos (i)$$

$d\Omega/dt$ must be positive which implies that "i" must be larger than 90°. So, the orbit is only near polar and is retrograde, the component of the rotation of the precessional mechanism about the Earth's axis being in the opposite direction to the Earth'rotation. The equatorial crossing time is fixed by the launch condition or by the subsequent post-launch adjustment.

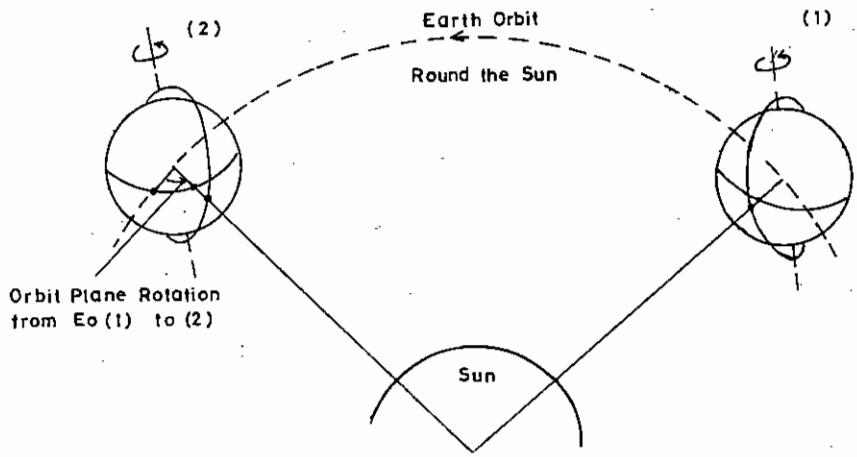


*Figure B. Orbital Precession to Achieve a Sun-synchroneous Orbit*